

## Endotoxin Inhibits Intestinal Epithelial Restitution through Activation of Rho-GTPase and Increased Focal Adhesions\*

Received for publication, December 12, 2003, and in revised form, March 5, 2004  
Published, JBC Papers in Press, March 30, 2004, DOI 10.1074/jbc.M313620200

Selma Cetin‡, Henri R. Ford‡§, Laura R. Sysko¶, Charu Agarwal\*\*, James Wang\*\*,  
Matthew D. Neal‡, Catherine Baty¶, Gerard Apodaca‡§§, and David J. Hackam‡¶¶

From the ‡Division of Pediatric Surgery, Department of Surgery, Children's Hospital of Pittsburgh and University of Pittsburgh, Pittsburgh, Pennsylvania 15213 and the ¶Center of Biologic Imaging, the ¶Department of Cell Biology and Physiology, the \*\*Department of Orthopedic Surgery, Department of Surgery, and the ‡‡Department of Medicine, University of Pittsburgh, Pittsburgh, Pennsylvania 15213

Diseases of gut inflammation such as neonatal necrotizing enterocolitis (NEC) result after an injury to the mucosal lining of the intestine, leading to translocation of bacteria and endotoxin (lipopolysaccharide). Intestinal mucosal defects are repaired by the process of intestinal restitution, during which enterocytes migrate from healthy areas to sites of injury. In an animal model of NEC, we determined that intestinal restitution was significantly impaired compared with control animals. We therefore sought to determine the mechanisms governing enterocyte migration under basal conditions and after an endotoxin challenge. Here we show that the cytoskeletal reorganization and stress fiber formation required for migration in IEC-6 enterocytes requires RhoA. Enterocytes were found to express the endotoxin receptor Toll-like receptor 4, which served to bind and internalize lipopolysaccharide. Strikingly, endotoxin treatment significantly inhibited intestinal restitution, as measured by impaired IEC-6 cell migration across a scraped wound. Lipopolysaccharide was found to increase RhoA activity in a phosphatidylinositol 3-kinase-dependent manner, leading to an increase in phosphorylation of focal adhesion kinase and an enhanced number of focal adhesions. Importantly, endotoxin caused a progressive, RhoA-dependent increase in cell matrix tension/contractility, which correlated with the observed impairment in enterocyte migration. We therefore conclude that endotoxin inhibits enterocyte migration through a RhoA-dependent increase in focal adhesions and enhanced cell adhesiveness, which may participate in the impaired restitution observed in experimental NEC.

Necrotizing enterocolitis (NEC)<sup>1</sup> is the leading cause of death from gastrointestinal disease in neonates and is second to

respiratory disease as the overall leading cause of morbidity and mortality in this population (1–3). Clinical manifestations of NEC include abdominal distention, feeding intolerance, and systemic sepsis, which result from the destruction of the intestinal barrier (4, 5). Mucosal breakdown may occur as a result of a perinatal insult, such as hypoxia, which allows bacteria and bacterial by-products to breach the normally impermeable mucosal barrier and initiate a local and systemic inflammatory response (4, 6, 7, 9). This causes the release of proinflammatory cytokines, including tumor necrosis factor, platelet-activating factor, nitric oxide, and endotoxin, which lead to further epithelial injury (10–13). Following mucosal damage, healing occurs initially through the process of epithelial restitution, in which healthy enterocytes adjacent to the sites of injury migrate toward the denuded mucosa to bridge the defect (14–18). We hypothesize that the intestinal barrier defect in NEC does not result from epithelial injury alone but also from impaired restitution. This paper focuses specifically on the process of enterocyte migration, which is the *sine qua non* of epithelial restitution and mucosal healing.

Although a variety of cytokines may be important in the initiation and propagation of the intestinal injury, endotoxin (lipopolysaccharide (LPS)) is likely to act at one of the earliest time points. LPS is one of the most abundant proinflammatory stimuli in the gastrointestinal tract, and a break in the mucosal barrier leads to translocation of LPS and a sustained LPS challenge (19, 20). This has direct local effects on the mucosal cells, including activation of the enterocytes (21–24), as well as systemic effects with activation of immune cells (25, 26). Sustained inhibition of epithelial restitution by LPS would lead to further bacterial translocation, potentiation of the inflammatory response, and further epithelial injury. Importantly, the effects of LPS on enterocyte migration and epithelial restitution remain largely unexplored.

The mechanisms governing enterocyte migration under basal conditions remain largely undefined. In other mammalian cells, migration is regulated by RhoA-GTPase, a member of the RhoA family of small molecular weight GTPases (27). Activation of RhoA leads to the subsequent activation of Rho kinase, leading to the formation of stress fibers that contract to pull the cell along the extracellular matrix (28). Although a role for RhoA in enterocyte migration has been postulated, its precise role in mediating enterocyte movement has not been definitively established, and the effects of endotoxin on RhoA activity in enterocytes remain unknown (29). Moreover, the ability of enterocytes to migrate during conditions of high endotoxin exposure, as would be expected during the systemic endotoxemia of NEC, remains unknown. A requirement for enterocytes to respond to endotoxin is the presence of the LPS receptor,

\* The costs of publication of this article were defrayed in part by the payment of page charges. This article must therefore be hereby marked "advertisement" in accordance with 18 U.S.C. Section 1734 solely to indicate this fact.

§ Supported by National Institutes of Health (NIH) Grants R01 AI-49473-01 and R01-AI-14032-20.

§§ Supported by NIH Grant R01 DK51970-06.

¶¶ Supported by NIH Grant K08 GM65583-01. To whom correspondence should be addressed: Division of Pediatric Surgery, Rm. 4A-486 DeSoto Wing, Children's Hospital of Pittsburgh, 3705 Fifth Ave., Pittsburgh, PA 15213. Tel.: 412-692-8735; Fax: 412-692-8299; E-mail: david.hackam@chp.edu.

<sup>1</sup> The abbreviations used are: NEC, necrotizing enterocolitis; LPS, lipopolysaccharide; TLR4, Toll-like receptor 4; GFP, green fluorescent protein; FAK, focal adhesion kinase; LPA, lysophosphatidic acid; fLPS, Alexa Fluor 488-labeled LPS; BrdUrd, bromodeoxyuridine; PI3K, phosphatidylinositol 3-kinase; GTP $\gamma$ S, guanosine 5'-3-O-(thio)triphosphate.

Toll-like receptor 4 (TLR4) (30, 31). Although TLR4 was recently found to be expressed by an enterocyte cell line (32), no direct role for enterocyte Toll proteins has been established, and a link between TLR4 and intestinal restitution remains to be examined.

In the current study, we show that intestinal restitution is impaired in an experimental model of necrotizing enterocolitis. We demonstrate that enterocytes express functional TLR4 and demonstrate that stress fiber formation, cell matrix adhesion, and migration in enterocytes require the activity of RhoA. Subsequently, we determine that LPS inhibits enterocyte migration by increased focal adhesion formation and enhanced cell matrix adhesion.

#### MATERIALS AND METHODS

**Cell Culture, Transfection, and Treatment**—IEC-6 and J774 cells were obtained from ATCC and maintained as described (33, 34). Where indicated, cells were treated with LPS (0.1–50  $\mu\text{g/ml}$  for 6 h; Cell Science (Norwood, MA) in the presence of LPS-binding protein (10 ng/ml; Cell Science). Control experiments showed that addition of LPS-binding protein alone had no effect on RhoA activation, cell migration, cell matrix tension, or cell morphology. To inhibit RhoA, cells were pretreated with C3 exotoxin from *Clostridium botulinum* (1  $\mu\text{g/ml}$ ; List Biological Inc., Campbell, CA) using LipofectAMINE 2000 (Invitrogen) as a carrier molecule 24 h prior to cell harvest, as described (35). Transient transfection of IEC-6 cells with GFP-tagged constructs of RhoA was performed using LipofectAMINE 2000 according to the manufacturer's protocol. Cells were used in all cases 24 h after transfection. Rabbit polyclonal antibodies to FAK and phospho-FAK were from Biosource (Camarillo, CA), anti-paxillin was from Upstate (Waltham, MA), and TLR4 was from Santa Cruz Biotechnology, Inc. (Santa Cruz, CA). Lysophosphatidic acid (LPA, 100  $\mu\text{M}$ ), Y27632 (10  $\mu\text{M}$ ), and LY294002 (100  $\mu\text{M}$ ) were from Calbiochem. Alexa Fluor 488-conjugated LPS from *Escherichia coli* O55:B5 was from Molecular Probes, Inc. (Eugene, OR). Cell viability was measured using trypan blue exclusion. GFP-tagged constructs encoding dominant negative, wild type, and constitutively active RhoA were the generous gifts of Dr. Guillermo Rimerio (University of Pittsburgh), Dr. Joseph T. Barbieri (Medical College of Wisconsin), and Dr. Michael S. Kolodny (UCLA School of Medicine).

To measure RhoA activation, we used the rhotekin binding domain affinity precipitation assay for RhoA-GTP according to the manufacturer's protocol (Cytoskeleton, Denver, CO) as described (36, 37). SDS-PAGE was performed as described (38). To assess TLR4 expression in intestine, fresh samples of either the terminal ileum or the ascending colon were obtained immediately after rats were sacrificed after 4 days of breast feeding (see animal model, below). After irrigation of the bowel to remove luminal contents, the mucosa was separated from the underlying connective tissue under a dissecting microscope and placed in cold lysis buffer (62.5 mM Tris, pH 6.6, 10% glycerol, 1% SDS, 0.5 mM phenylmethylsulfonyl fluoride, 2  $\mu\text{g/ml}$  aprotinin, and 10  $\mu\text{g/ml}$  leupeptin), homogenized, and boiled for 1 min. Histologic evaluation of scraped tissue confirms that it is composed predominantly of enterocytes, with small numbers of contaminating lymphocytes (data not shown). Bands were detected with enhanced chemiluminescence (ECL-Super Signal, Pierce), and images on radiographic film were quantified using a GS700 Bio-Rad densitometer and QuantityOne analysis software (Hercules, CA). For immunofluorescence, cells or tissue were processed as described (39, 40), and fluorescent images were captured using an Olympus Fluoview500 confocal microscope under a 60 $\times$  oil immersion objective using standard filter sets. To assess the subcellular distribution of GFP-tagged RhoA constructs, transfected cells were fixed as above, mounted, and viewed under fluorescein isothiocyanate filter sets. To evaluate the uptake of LPS, IEC-6 cells were incubated with Alexa Fluor 488-labeled LPS (fLPS) (1 ng/ml) for 1 h at 37  $^{\circ}\text{C}$ . To block TLR4, IEC-6 cells were pretreated with anti-TLR4 (1:50) for 1 h at 4  $^{\circ}\text{C}$  prior to treatment with fLPS. In parallel, IEC-6 cells were pretreated with Alexa Fluor 488-conjugated human transferrin (5  $\mu\text{g/ml}$ , 2 h, 37  $^{\circ}\text{C}$ ; Molecular Probes) in the presence and absence of anti-TLR4. Where indicated, the location of the nuclei in fixed, permeabilized cells or tissue was demonstrated using TOPRO-3 (1:1000, Molecular Probes). Digital images were prepared and labeled using Adobe Photoshop<sup>®</sup> 7.0 software.

**Determination of Enterocyte Migration and Intestinal Restitution**—IEC-6 cells were grown on glass coverslips to 100% confluence then serum-starved for 12 h, scraped with a cell scraper, and then transferred to the stage of an Olympus 1X71 inverted microscope (Melville,

NY) and perfused with Dulbecco's modified Eagle's medium plus 10 mM Hepes, pH 7.4, at 0.5 ml/h. Images were taken every 5 min for 18 h and analyzed using Metamorph software (Universal Imaging Corp., Downingtown, PA). A calibration scale was obtained, and the migration rate was determined by measuring the mean distance traveled by 15 cells/field over the course of the experiment. Measurements were obtained from cells that were selected both at the leading edge and several rows back.

For measurements of intestinal restitution, the experimental protocol was approved by the Animal Research and Care Committee of the Children's Hospital of Pittsburgh. Necrotizing enterocolitis was induced in newborn rat pups by administration of enteral formula and induction of hypoxia (5% oxygen for 10 min prior to each feeding) three times daily as in Ref. 41. Animals were sacrificed on day 4, and samples of the terminal ileum revealed inflammatory characteristics of necrotizing enterocolitis, including neutrophil infiltration, edema of the lamina propria, and mucosal ulceration (41). Control animals remained with their mothers and received breast milk. To measure enterocyte migration, animals with established NEC or controls were injected with bromodeoxyuridine (50 mg/kg 5'-BrdUrd; Sigma) intraperitoneally and then sacrificed either 1 or 18 h later. Samples of terminal ileum were then immunostained using anti-BrdUrd antibodies as described (42). Enterocyte migration was expressed by 1) measuring the distance from the bottom of the crypt to the foremost labeled enterocyte and 2) expressing the distance as a percentage of total villus height.

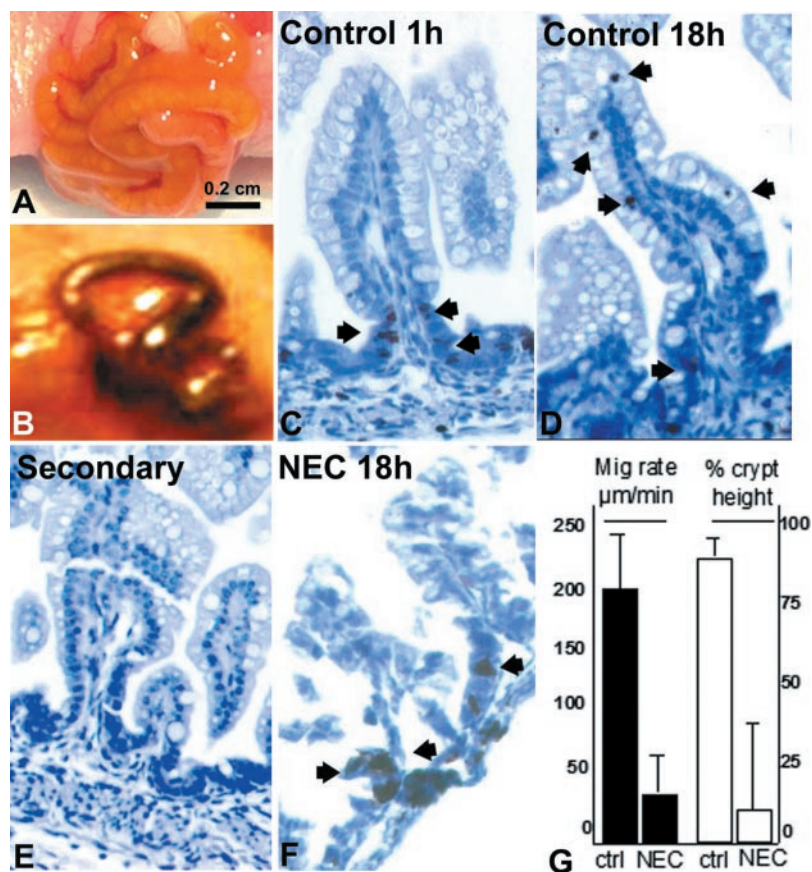
**Assessment of Cell Matrix Tension**—Two techniques were utilized to measure cell matrix tension. The first is based upon the methodology of Grinnell *et al.* (43). IEC-6 cells ( $2 \times 10^6$ ) were plated on top of collagen matrices that were formed in 6-well plates (~98% bovine collagen type I; Cohesion Technologies Inc.), 0.1 M NaOH, and 10 $\times$  phosphate-buffered saline mixed together in an 8:1:1 ratio). After 24 h at 37  $^{\circ}\text{C}$ , collagen discs were gently lifted from the wells using a scraper ( $t = 0$  h) and treated with fresh media and LPA (100  $\mu\text{M}$ ), LPS (50  $\mu\text{g/ml}$ ), or C3 exotoxin (1  $\mu\text{g/ml}$ ) for 24 h to allow contraction to occur ( $t = 24$  h). Contraction was determined by measuring the change in diameter of the gel over the 24-h period using a ruler by two independent observers. The second technique utilized a culture force monitor system, as described by Campbell *et al.* (44). Briefly, enterocyte-collagen matrices were prepared as above, and the solution was pipetted into silicon dishes in the presence of LPA (100  $\mu\text{M}$ ), LPS (50  $\mu\text{g/ml}$ ), or LPA plus Y27632 (10  $\mu\text{M}$ ). As the enterocytes exerted tension, they contracted the collagen gel, which displaced a detector attached to a semiconductor strain gauge. The resulting change in voltage was recorded using the Labview software program for 10 s, every 10 min where each data point corresponded to the average of 100 samples. In all cases, no tension was generated in the absence of enterocytes, and equal numbers of IEC-6 cells were used in each group ( $2 \times 10^6$ ).

**Statistics**—Data presented are mean  $\pm$  S.E. Comparisons are by two-tailed Student's *t* test, with statistical significance accepted for  $p < 0.05$ .

#### RESULTS

**Intestinal Restitution Is Impaired in Experimental Necrotizing Enterocolitis**—We hypothesized that NEC is associated with impaired epithelial restitution. To measure this directly, we examined the rate and extent of intestinal restitution in a neonatal rat model of gut inflammation that resembles human NEC (41). The combination of hypoxia and enteral formula consistently caused severe morphologic changes in the small intestine. Compared with the pink, healthy small intestine of control animals (Fig. 1A), animals with experimental NEC developed patchy intestinal necrosis, edema, and marked friability of the intestinal wall (Fig. 1B). To determine whether these changes were associated with impaired enterocyte migration, rats were injected in both groups with an intraperitoneal bolus of 50 mg/kg BrdUrd at 1 or 18 h before death. An analysis of over 50 serial sections at 1 h indicated that the percentage of labeled crypt cells was similar in both groups (percentage of BrdUrd-positive crypt cells compared with control:  $10 \pm 3\%$  versus NEC,  $12 \pm 5\%$ , not significant). The majority of the BrdUrd uptake in control animals at 1 h is localized to the crypts (see the arrows in Fig. 1C), whereas by 18 h a significant proportion of the staining had traveled along the villus and even reached the tips in some cases (Fig. 1D, arrows). By

**FIG. 1. Epithelial restitution is impaired in experimental necrotizing enterocolitis.** Necrotizing enterocolitis was induced in newborn rats that were subjected to 4 days of enteric formula and systemic hypoxia three times daily. Control animals remained with their mothers and were breast-fed. Compared with the appearance of the small intestine of control animals (A), this treatment caused intestinal inflammation, edema, and necrosis similar to that observed in human necrotizing enterocolitis. B, to assess enterocyte migration along the crypt-villus axis, control (C–E) and NEC animals (F) were injected with BrdUrd 1 h (C) and 18 h (D–F) prior to sacrifice and then immunostained for BrdUrd (the arrows indicate position of peroxidase staining). At 1 h following injection, most of the uptake is observed in the intestinal crypts (C, the arrows show BrdUrd-positive cells), whereas at 18 h, most has accumulated at varying positions along the villi (D, arrows). The specificity of the staining is confirmed by the lack of staining when secondary antibody alone is used (E). In NEC animals, the majority of the BrdUrd uptake remains in the crypts (F), demonstrating a significant impairment in migration. The rate of migration and the percentage of the maximal crypt height achieved by migrating enterocytes is significantly decreased in NEC animals compared with controls (G). Data are means  $\pm$  S.E. of three experiments. A minimum of 100 cells was counted per experiment.



contrast, in animals with NEC, the majority of the staining remained in the crypts even by 18 h (Fig. 1F, arrows). Both the rate and extent of intestinal restitution (enterocyte migration) were significantly reduced in rats with NEC compared with control animals (Fig. 1G). The impaired intestinal restitution in NEC occurred independent of the degree of mucosal deformation by the inflammatory process (note the lack of progression of BrdUrd-positive enterocytes in both villi in Fig. 1F). Together, these data indicate that NEC is associated with significant impairment in intestinal restitution and enterocyte migration along the crypt-villus axis.

**Enterocytes Express the LPS Receptor TLR4, Which Mediates the Binding of Endotoxin**—In order to assess the effects of endotoxin (LPS) on enterocyte migration, we examined the expression of the LPS receptor TLR4 in enterocytes. As is shown in Fig. 2A, IEC-6 enterocytes were found to express TLR4 by SDS-PAGE, at a molecular weight similar to that of the TLR4 expressed in J774 macrophages. To ensure that TLR4 expression was not solely a feature of the IEC-6 cell line, we next sought to determine whether primary enterocytes express TLR4. Because primary enterocyte cell lines are difficult to establish, we used a method of mucosal dissection to prepare enterocytes from the intestine of newborn rats on day 4 of life. The resulting tissue is composed predominantly of enterocytes, with a very small number of contaminating intraepithelial lymphocytes (data not shown). As shown in Fig. 2A, enterocytes from both the terminal ileum and ascending colon were found to express TLR4. The subcellular distribution of TLR4 in IEC-6 cells as evaluated by indirect immunofluorescence and confocal microscopy is shown in Fig. 2B. The specificity of the antibody staining in these studies is supported by studies performed in two cell lines that are TLR4-deficient (cortical collecting duct cells and human embryonic kidney cells (45)) in which there was no detectable TLR4 staining (data not shown). To investi-

gate whether TLR4 could function in the binding of LPS by enterocytes, IEC-6 cells were incubated with fluorescein-conjugated LPS in the presence and absence of anti-TLR4 antibodies or an irrelevant IgG. In control cells, LPS appeared both at the plasma membrane and within the cytoplasm (Fig. 2, C and D). By contrast, pretreatment of cells for 1 h with anti-TLR4 antibodies completely prevented LPS uptake (Fig. 2, E and F). Pretreatment with an irrelevant antibody had no effect (data not shown). Anti-TLR4 antibodies were not acting to nonspecifically inhibit endocytosis, since there was no effect on the uptake of Alexa Fluor 488-conjugated human transferrin by enterocytes (Fig. 2, G and H). Finally, to assess the expression of TLR4 in the intestinal mucosa histologically, samples of terminal ileum were obtained from 6-week-old rats, immunostained with anti-TLR4 antibodies, and assessed by confocal microscopy. TLR4 was detected on the enterocytes (Fig. 2I, see inset for higher magnification, in which the arrows point to the TLR4 expression). Treatment of tissue with secondary antibody alone revealed no staining, highlighting the specificity of these findings (Fig. 2H). Together, these data indicate that enterocytes express TLR4 and that this receptor may participate in LPS binding.

**Lipopolysaccharide Significantly Impairs Enterocyte Migration**—We next investigated the effects of LPS on enterocyte migration *in vitro* by assessing the ability of confluent IEC-6 cells to reconstitute a scraped wound. Representative digital micrographs from a typical migration experiment with control (Fig. 3, A and B) and LPS-treated (Fig. 3, C and D) cells are shown. In control cells, the wound was completely closed by 12 h (Fig. 3B). By contrast, LPS-treated cells revealed a significant inhibition in the rate of migration and a consistent inability to close the wound at any time point (Fig. 3, C and D). There was no effect of LPS on cellular viability after 12 h of treatment (percentage viability in control:  $80 \pm 10\%$  versus

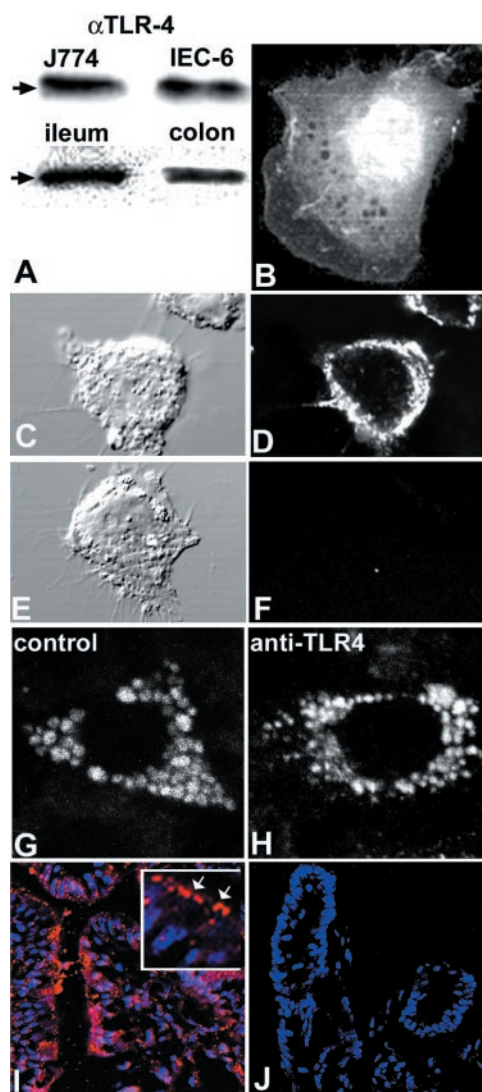


**FIG. 2. Enterocytes express the endotoxin receptor, TLR4, which mediates LPS binding and uptake.** *A*, lysates were prepared from J774 macrophages, IEC-6 enterocytes, and mucosal scrapings from the ileum and colon of newborn rats and then separated by SDS-PAGE on a 10% gel, transferred to polyvinylidene difluoride, and probed by immunoblotting with affinity-purified polyclonal antibodies to TLR4. Identical amounts of protein (20  $\mu$ g) were used in all lanes. Two blots are shown; the *arrows* indicate the location of the 97-kDa molecular mass standard. Results are representative of four similar determinations. *B*, IEC-6 cells were fixed, permeabilized, blocked, and then immunostained with anti-TLR4 primary antibodies followed by Alexa Fluor 488 anti-rabbit secondary antibody and the nuclear stain TOPRO-3. The subcellular distribution of TLR4 was determined using fluorescence confocal microscopy. A representative grayscale image of a cell showing the merged TOPRO-3 staining and TLR4 staining is shown. *C–F*, IEC-6 cells were incubated with fLPS and then analyzed by differential interference contrast (*C*) and fluorescence confocal microscopy (*D*), revealing uptake of fLPS. IEC-6 cells were pretreated with anti-TLR4 antibodies for 1 h at 4 °C and then treated with fLPS and analyzed by differential interference contrast (*E*) and fluorescence confocal microscopy (*F*), revealing inhibition of fLPS uptake. Images are representative of three similar experiments. *G* and *H*, IEC-6 cells were allowed to internalize Alexa Fluor 488-conjugated human transferrin in the absence (*G*) or presence (*H*) of pretreatment with anti-TLR4 antibodies, and the distribution of transferrin is shown by confocal microscopy. *I*, distal ileum was harvested from newborn rats and immunostained with anti-TLR4 (*red*) and TOPRO-3 (*blue*). Size bar, 100  $\mu$ m. At higher magnification, the distribution of TLR4 is seen (*inset*, *arrows*). *J*, terminal ileum treated as in *I* without the addition of the primary antibody, revealing nuclear staining alone.

LPS,  $75 \pm 5\%$ ,  $n = 10$ , not significant). The rates of migration and the effects of increasing doses of LPS are summarized in Fig. 3*E*. Together, these data indicate that LPS significantly

impairs enterocyte migration *in vitro*.

**RhoA Is Required for Formation of Stress Fibers in Enterocytes**—We next sought to understand the mechanisms governing intestinal restitution by enterocyte migration. In many mammalian cells, migration requires actin stress fibers that form in response to activation of RhoA (46). Transfection of IEC-6 cells with wild-type RhoA caused no change in stress fiber morphology (Fig. 4, *A* and *B*), whereas transfection with dominant negative mutants caused a significant disruption in stress fibers (Fig. 4, *C* and *D*; *arrows* point to transfected cells). Treatment of cells with the RhoA inhibitor C3 exotoxin (Fig. 4*E*) and the Rho kinase inhibitor Y27632 (Fig. 4*F*) both caused a marked disruption in stress fibers. These data indicate that RhoA is required for stress fiber formation in enterocytes and suggest a potential role for RhoA in enterocyte migration. To test this further, we examined whether pharmacologic activation of RhoA would affect the rate or extent of enterocyte migration. Confluent, serum-starved IEC-6 cells were treated with LPA, which activates RhoA, and then assessed for their ability to migrate. As is shown in Fig. 3*E*, LPA treatment significantly decreased enterocyte migration compared with control cells. These data demonstrate that stress fiber formation requires RhoA activity in enterocytes and that RhoA activation is associated with impaired enterocyte migration. We therefore next sought to assess the effects of LPS on RhoA activity.

**LPS Increases RhoA Activity in a PI3K-dependent Manner in Enterocytes**—RhoA activity in enterocytes after endotoxin treatment was assessed using a pull-down assay as described (36, 37). To assess the proportion of “active” (*i.e.* GTP-bound) RhoA, IEC-6 cell lysates were incubated with glutathione beads that had been conjugated to rhotekin, a molecule that selectively binds to active RhoA (*Active Rho* in Fig. 5, *A* and *C*). Analysis of the proportion of RhoA bound to the beads compared with the total cellular content of RhoA by SDS-PAGE (*Total Rho* in Fig. 5, *A* and *C*) provides a measure of the percentage of activated RhoA in the cell. To validate this assay, IEC-6 cells were treated with the RhoA activator LPA, which caused an increase in RhoA activity (Fig. 5, *A* and *B*). As a positive control for rhotekin binding to GTP-RhoA, lysates were treated with GTP $\gamma$ S (0.2 mM, 1 h), which yielded a band of maximal intensity compared with all other treatment groups (Fig. 5, *A* and *C*). Strikingly, LPS treatment of IEC-6 cells resulted in a significant increase in activated RhoA compared with untreated cells (Fig. 5, *A* and *B*). The specificity of the assay was confirmed by pretreating IEC-6 cells with C3 exotoxin. This significantly decreased RhoA activity and blocked the LPS-induced increase in RhoA activation (Fig. 5, *C* and *D*).

We next sought to understand the molecular pathway leading to the activation of RhoA by LPS in enterocytes. Because RhoA activation has been shown to require PI3K in other cells (47), we next investigated whether PI3K was required for the endotoxin-induced activation of RhoA in enterocytes. In a series of preliminary experiments, we determined the effective concentration of the PI3K inhibitor LY294002 in IEC-6 cells by showing that a concentration of 100  $\mu$ M was required to prevent the activation of AKT by epidermal growth factor (data not shown). Pretreatment of IEC-6 cells with LY294002 did not influence the expression of total cellular RhoA, yet it significantly inhibited the activation of RhoA by LPS (Fig. 5, *A* and *B*). RhoA becomes membrane-associated in the activated state, and the degree to which this occurs correlates with the extent of its activation. To further validate the LPS responsiveness of enterocytes (48, 49), we sought to confirm that endotoxin activates RhoA in IEC-6 cells by investigating the subcellular distribution of RhoA in the presence or absence of LPS. RhoA was

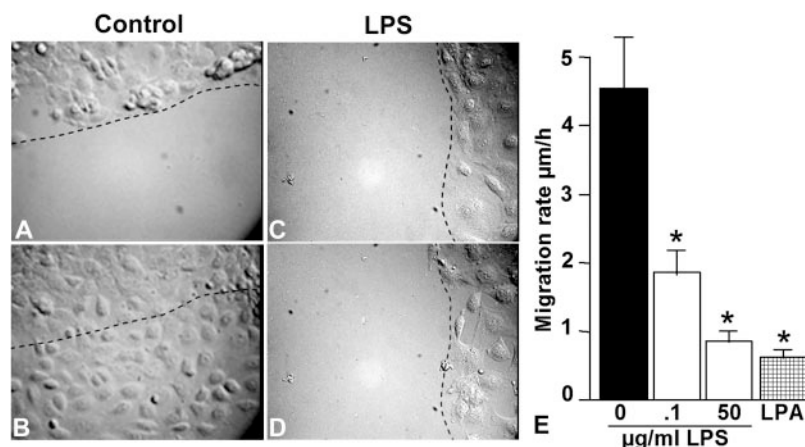


**FIG. 3. Lipopolysaccharide significantly impairs enterocyte migration.** Confluent IEC-6 cells were plated on glass coverslips, scraped with a cell scraper, and then mounted on the stage of an Olympus 1X71 inverted microscope warmed to 37 °C. Fresh medium was continuously perfused across the cells in the presence or absence of LPS and LPS-binding protein at the indicated concentration. Differential interference contrast images were obtained every 5 min. Shown are images from a typical experiment of the migration of control IEC-6 cells, where the *dotted line* indicates the position of the cells at the edge of the scraped wound. Digital images were obtained in control cells at  $t = 0$  (A) and  $t = 12$  h (B), revealing complete wound closure and in LPS (50 µg/ml)-treated IEC-6 cells at  $t = 0$  (C) and  $t = 12$  h (D), revealing inhibited wound closure as a result of impaired migration. E, quantification of migration rate, calculated as the mean distance traveled by 50 individual cells in an orientation perpendicular to the axis of the scrape over the time course of the experiment. Data are means  $\pm$  S.E. of 10 experiments. \*,  $p < 0.05$  compared with no LPS.

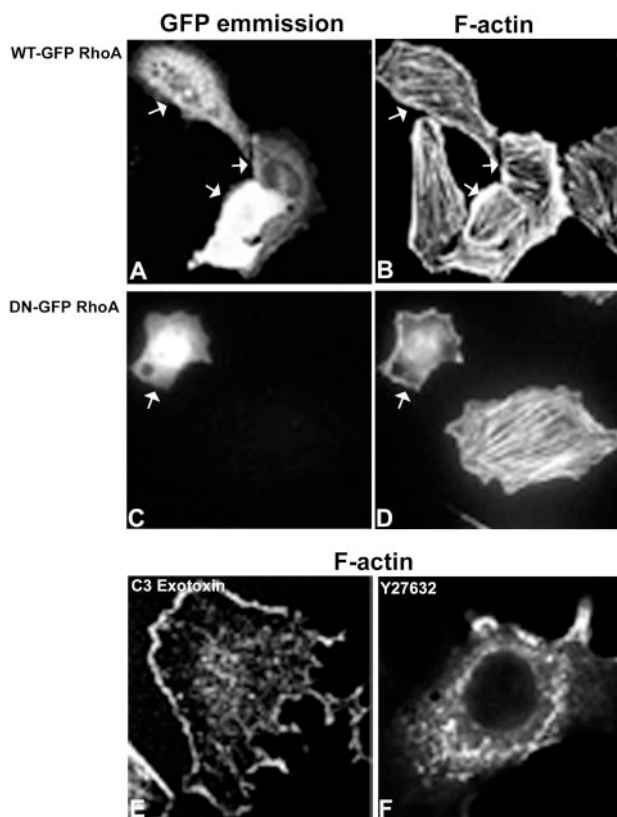


**FIG. 4. RhoA is required for stress fiber formation in enterocytes.** A–D, IEC-6 cells were transiently transfected with GFP-wild type RhoA (A and B) or GFP-N17 (dominant negative) RhoA (C and D) 24 h before analysis, and F-actin distribution was assessed by rhodamine-phalloidin staining. Cells were then visualized by fluorescence confocal microscopy. A and C, GFP staining; B and D, phalloidin staining. The *arrows* indicate transfected cells. Note the inhibition of stress fibers by dominant negative but not wild type RhoA. E and F, IEC-6 cells were treated with C3 exotoxin (E) or the Rho kinase inhibitor Y27632 (F) and then stained with rhodamine-phalloidin. Note the loss of stress fibers. A representative cell is displayed under each condition. All experiments were repeated at least five times.

detected in serum-starved control IEC-6 cells in a diffuse, cytoplasmic pattern (see Fig. 6A for a representative cell). By contrast, treatment of cells with LPS caused a redistribution of

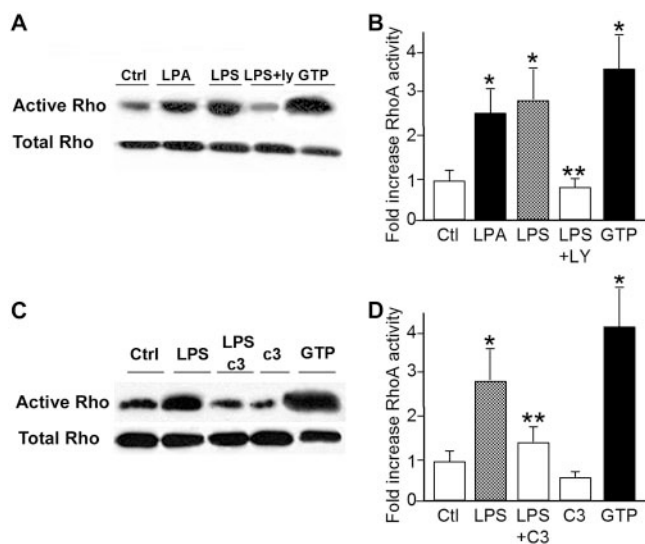


**FIG. 5. Lipopolysaccharide increases the activity of RhoA in enterocytes.** A, whole cell lysates were purified from serum-starved IEC-6 cells that had been treated as described under “Materials and Methods”: *Ctrl*, *LPS*, *LPS+ly*, and *GTP* (as a positive control for RhoA-GTPase activation, lysates were incubated with 0.2 mM GTP $\gamma$ S for 1 h at 37 °C). Lysates were then subjected to the rhotekin pull-down assay described under “Materials and Methods.” The GST-rhotekin beads (*Active RhoA*), which reflect the total activated RhoA in the cell lysates, and 20 µg of the whole cell lysates (*Total Rho*) in each group were then separated by SDS-PAGE, transferred to polyvinylidene difluoride membranes, and immunoblotted with anti-RhoA antibodies. B, densitometry data from A expressed in integrated optical density units of RhoA-GTP/total RhoA as a percentage of control for each experiment (\*,  $p < 0.05$  compared with control; \*\*,  $p < 0.05$  compared with LPS,  $n = 8$  separate experiments). C, lysates were prepared as in A above but were treated under the following conditions as described under “Materials and Methods”: *LPS*, *LPS+C3*, *C3*, and *GTP*. D, densitometry data from C, where the *ordinate* indicates band density relative to control. \*,  $p < 0.05$  compared with control; \*\*,  $p < 0.05$  compared with LPS,  $n = 7$  separate experiments. Representative blots are displayed.

RhoA to a perinuclear location (Fig. 6B), which closely resembled the pattern obtained after treatment with LPS (Fig. 6C). To confirm that the extent of RhoA activation influences its subcellular distribution, we examined the localization of GFP-constitutively active RhoA in IEC-6 cells in comparison with

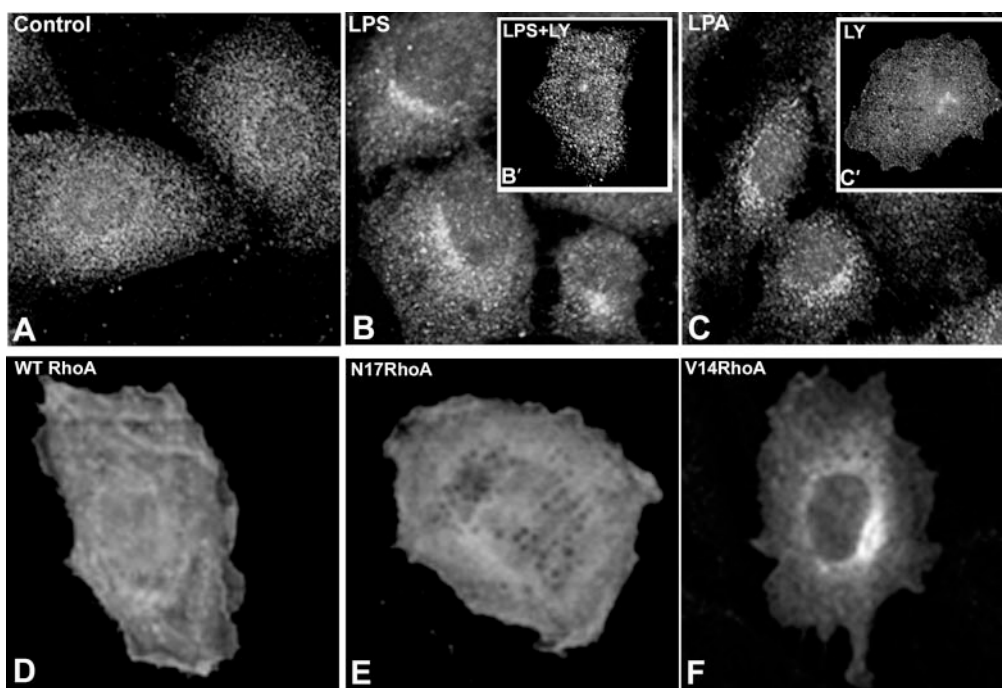


**FIG. 6. LPS treatment of enterocytes results in a shift in the subcellular distribution of RhoA from a cytosolic to a perinuclear compartment.** A–C, serum-starved IEC-6 cells were treated with LPA or LPS as described under “Materials and Methods” and then immunostained for RhoA and examined by fluorescence confocal microscopy. Representative samples from five separate experiments are displayed. A, control cells; B, LPS-treated cells (*inset B'* shows cell treated with LPS + LY294002); C, LPA-treated cells, showing accumulation of RhoA in a perinuclear pattern after RhoA activation (*inset C'* shows the effect of LY294002 alone). D–F, IEC-6 cells were transiently transfected with GFP-tagged constitutively active, dominant negative N19RhoA or constitutively active V14RhoA constructs, fixed in paraformaldehyde, and then examined for GFP fluorescence using confocal microscopy. D, representative wild type RhoA-transfected cell; E, representative dominant negative RhoA-transfected cell; F, representative constitutive active RhoA-transfected cell revealing the perinuclear accumulation of active GFP-RhoA.

both wild-type (GFP-V14RhoA) and dominant-negative (GFP-N19RhoA) constructs. Both wild-type and dominant negative RhoA constructs were detected in a diffuse pattern within the cytoplasm, similar to that of endogenous RhoA in control IEC-6 cells (see Fig. 6, D and E, for representative cells). By contrast, constitutively active GFP-V14RhoA appeared in a perinuclear distribution (Fig. 6F). This appearance was comparable with that of endogenous RhoA in the presence of LPS or LPA (Fig. 6, compare F with B and C). Importantly, treatment of IEC-6 cells with LPS in the presence of LY294003 completely prevented the redistribution of RhoA, which remained in a diffuse, cytoplasmic pattern (see Fig. 6B'). LY294002 treatment alone had no effect on RhoA activation (see Fig. 6C'). Taken together, these data indicate that LPS activates RhoA in a PI3K-dependent manner in enterocytes.

**Lipopolysaccharide Causes an Increase in Focal Adhesion Formation in Enterocytes**—For cells to migrate, they must first “loosen” their attachments with the underlying matrix (50). Cell attachment requires the formation of stress fibers and is mediated through focal adhesions. These are protein complexes that include paxillin and focal adhesion kinase, which is phosphorylated when activated (27, 51). Having shown that RhoA is required for stress fiber formation in enterocytes and is activated by LPS, we next sought to establish whether LPS increases focal adhesion formation. In control cells, phospho-FAK was detected at discrete focal adhesions that localized to the tips of actin stress fibers (Fig. 7A, *i–iii*). LPS treatment caused an increase in the density of phospho-FAK staining within the cell, which was found to colocalize with actin stress fibers (Fig. 7A, *iv–vi*), indicating an increase in focal adhesion formation. A similar effect was observed after LPA, further implying that the effects could be obtained by activating RhoA (Fig. 7A, *vii–ix*). Importantly, the effects of LPS on focal adhesion formation could be blocked by preincubation of cells with the PI3K

inhibitor LY294002 (Fig. 7A, *x–xii*). By SDS-PAGE, phospho-FAK (*pFAK*) expression was significantly increased after LPS treatment compared with untreated controls, with no effect on total FAK expression. Similar results were obtained after LPA treatment (Fig. 7B). Pretreatment of IEC-6 cells with anti-TLR4 antibodies prevented the LPS-mediated effects on phospho-FAK, indicating a requirement for TLR4 signaling (Fig. 7C). To confirm that focal adhesion formation was affected, LPS significantly increased paxillin density, and this effect was inhibited by LY294002 (Fig. 7D). Importantly, RhoA inhibition blocked the LPS-induced increase in phospho-FAK expression and decreased overall phospho-FAK immunostaining (Fig. 7E). Together, these findings indicate that LPS results in an increase in focal adhesion formation in enterocytes in a RhoA- and PI3K-dependent fashion. These data raise the possibility that the impairment in migration by LPS occurs as a result of exaggerated cell matrix adhesion.

**LPS Impairs Enterocyte Migration by Increasing Enterocyte Adhesion to the Underlying Cell Matrix**—Having shown that LPS treatment causes a marked increase in the distribution and extent of focal adhesions in enterocytes, we next investigated whether this was associated with an increase in the strength with which the enterocytes were attached to the underlying matrix, which could impair their ability to migrate. Direct measurements of cell matrix tension using two related techniques in which enterocytes were plated on collagen matrices are displayed in Fig. 8. Twenty-four hours after LPS or LPA treatment, there was a consistent decrease in the diameter of the gels, which reflects that cell matrix tension had been generated during the 24-h interval (Fig. 8, A and B). The change in diameter could be blocked by pretreating cells with C3 exotoxin, indicating the requirement of RhoA for this process (Fig. 8C). We next quantified the magnitude of the force generated by enterocytes as they interacted with the underly-

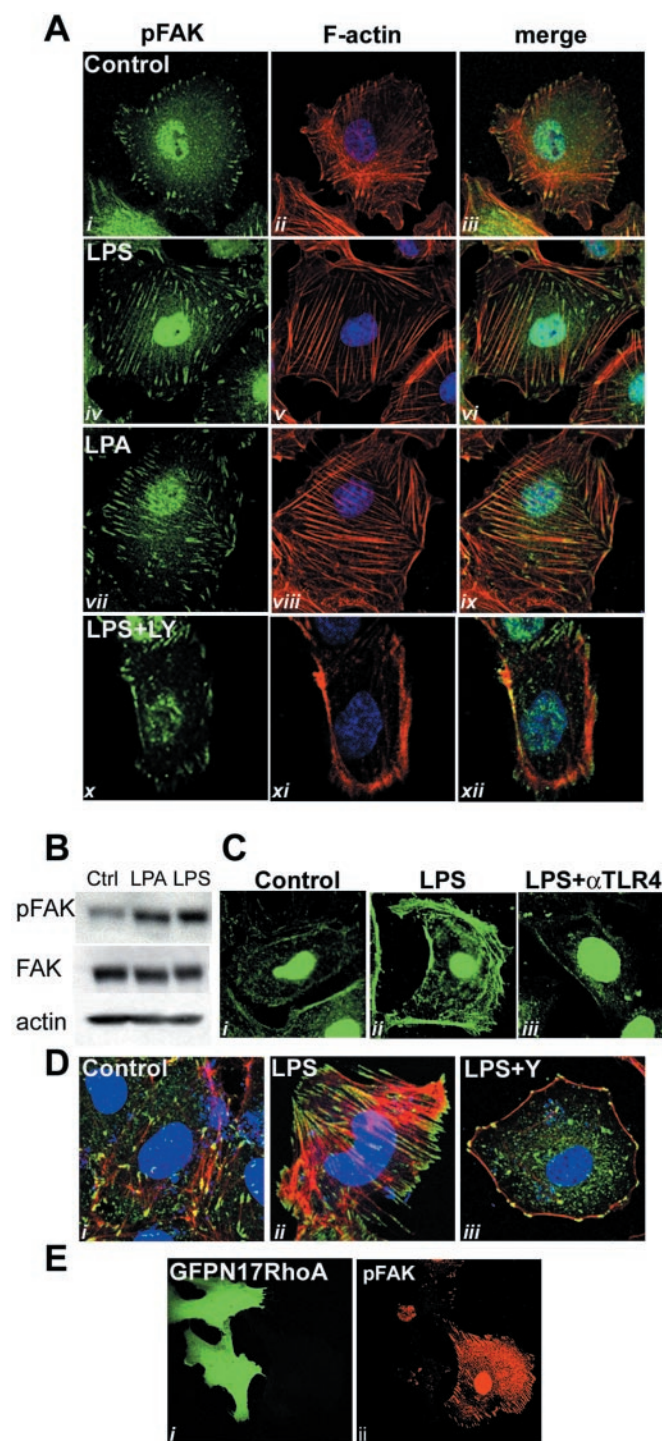


**FIG. 7. LPS increases focal adhesion formation in enterocytes.** A, serum-starved IEC-6 cells were treated in the absence (*i-iii*) or presence of LPS (*iv-vi*), LPA (*vii-ix*), or LPS + LY294002 (*x-xii*) and then immunostained for phospho-FAK (green) and actin (red) with the nuclear stain TOPRO-3 (purple). Cells were then analyzed by fluorescence confocal microscopy. Corresponding green and red/purple images were then overlaid (merge), such that sites at which phospho-FAK and actin labeling colocalize (*i.e.* focal adhesions) appear bright orange. B, whole cell lysates were obtained from serum-starved IEC-6 cells in the absence (*Ctrl*) or presence of LPA or LPS and then immunoblotted against phospho-FAK (20  $\mu$ g/lane). Blots were then stripped and re-probed for total FAK and then total actin. C, serum-starved IEC-6 cells were either untreated (*i*) or treated with LPS in the absence (*ii*) or presence (*iii*) of anti-TLR4 antibodies, immunostained with anti-phospho-FAK antibodies, and assessed by confocal microscopy. D, serum-starved IEC-6 cells were either untreated (*i*) or treated with LPS (*ii*) or LPS + Y27632 (*iii*) and then immunostained for paxillin (green) and actin using rhodamine phalloidin (red) and TOPRO-3 (purple). Corre-

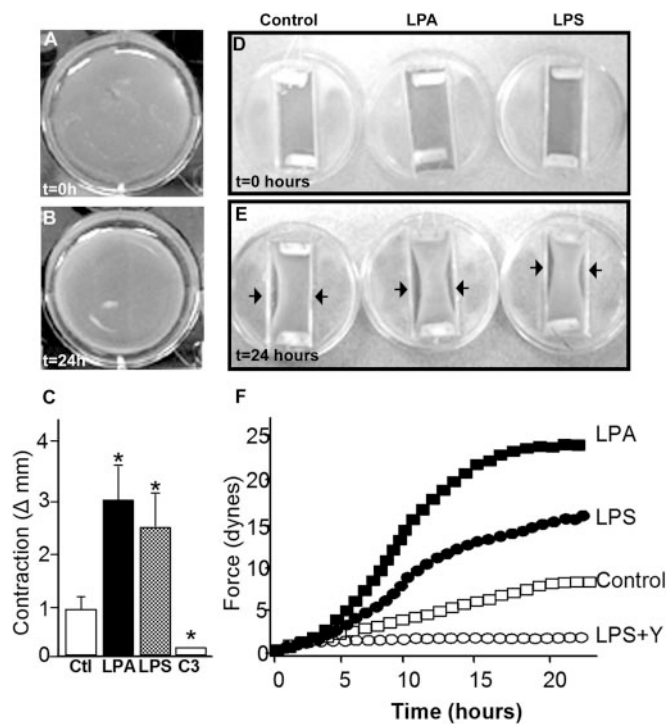


**FIG. 8. Effect of LPS on cell matrix tension in enterocytes.** A–C,  $2 \times 10^6$  IEC-6 cells were plated on the surface of collagen disks that were formed within 6-well plates. After 24 h at 37 °C to allow for cell matrix adhesion, disks were removed and placed in fresh medium in 6-well plates with the indicated treatment. Measurements of the diameter of the disks were taken at the time of placement into the new wells ( $t = 0$ ) (A) and 24 h later ( $t = 24$ ) (B), using a ruler. Shown is a representative image with LPS-treated cells where a 3-mm change in diameter was detected. C, quantification of gel contraction in control cells (*Ctl*) or in cells treated with LPA (*LPA*), LPS (*LPS*), or C3 exotoxin (*C3*). The ordinate represents the difference in millimeters between the diameter of the collagen disks at  $t = 0$  h and  $t = 24$  h. \*,  $p < 0.05$  compared with control cells. D–F,  $2 \times 10^6$  IEC-6 cells were placed within collagen gels and transferred to a contraction measurement device as described under “Materials and Methods.” Continuous measurements were recorded of the contraction generated by the cells in the absence (*control*) or presence of LPA, LPS, or LPS + Y27632, and data were graphed hourly. Representative images showing the appearance of the gels at the start of the experiment ( $t = 0$  h) (D) and after 24 h of contraction in E. The arrows denote points at which the cell contraction has resulted in a deformation in the shape of the gel, which was quantified in F, where the ordinate represents the force generated in dynes over time. Results are representative of more than 10 separate experiments.

ing matrix and the role of RhoA in this process (Fig. 8, D–F). A representative image depicting the appearance of the enterocyte-containing gels at the beginning (Fig. 8D) and at the end (Fig. 8E) of the gel contraction is shown. Gel contraction was most prominent across the midportion of the gels, resulting in the acquisition of an “hourglass” shape, where regions of maximal gel contraction are highlighted by the arrows in Fig. 8E. As quantified in Fig. 8F, maximal force was generated after treatment with the Rho-GTPase activator LPA. Strikingly, LPS treatment generated significant force compared with untreated cells. Treatment of IEC-6 cells with LPS in the presence

sponding green and red/purple images were then overlaid, and colocalization of paxillin and F-actin appears bright orange in the merged image. E, serum-starved IEC-6 cells were transfected with GFP-dominant negative RhoA 24 h prior to be treatment with LPS and then stained for phospho-FAK. Cells were analyzed by fluorescence confocal microscopy to display the GFP (*i*) and phospho-FAK (*ii*) staining. Three cells are displayed, two of which are transfected with GFP-DN RhoA and one of which is untransfected. Representative images from at least five separate experiments are displayed in each case.

of the Rho kinase inhibitor Y27632 completely prevented force generation, confirming that the generated force was Rho-dependent. Based upon these data, we conclude that endotoxin inhibits enterocyte migration by increasing the strength of the adhesiveness between the cells and the underlying cell matrix, in a RhoA-dependent manner.

#### DISCUSSION

Injury to the neonatal intestinal barrier, such as may occur after a hypoxic insult, leads to bacterial translocation and the development of necrotizing enterocolitis (33). The causal relationship between bacterial colonization of the intestine and the development of NEC is strong. NEC develops only after bacterial colonization of the gut has occurred and may be prevented through the use of prophylactic enteric antibiotics (53–55). This suggests that the interplay between bacteria and a damaged mucosal barrier is critical for the development of NEC. Following the translocation of bacteria and endotoxin, proinflammatory cytokines, including platelet-activating factor and nitric oxide, are released, leading to further mucosal injury (10, 12). The effects of either endotoxin or proinflammatory cytokines on the extent of intestinal restitution remain largely unexplored. We now show that LPS directly impairs mucosal healing by impairing enterocyte migration (Fig. 3). Other proinflammatory cytokines may act to impair enterocyte migration as well,<sup>2</sup> suggesting that the combined effects of the proinflammatory milieu adversely affect intestinal restitution. The current study focuses on the specific role of endotoxin, since it is expected to act much earlier than the other cytokines and is likely to be present at very high levels after bacterial translocation has occurred. Together, these findings broaden our understanding of the pathogenesis of intestinal injury by revealing that endotoxin and cytokines may not merely disrupt the intestinal barrier through cytotoxic effects but may also directly impair its capacity to heal. This notion is supported by previous experiments that demonstrate that endotoxin impairs enterocyte proliferation, which is required at later stages of mucosal healing (33).

It is noteworthy that the current data indicate that enterocytes are responsive to LPS (Figs. 5 and 6), which appears initially to contradict other studies that have concluded that enterocytes are unresponsive to endotoxin (48, 56, 57). This apparent conflict may be resolved by assessing the molecular pathways that have been examined. For instance, others have shown that LPS does not cause NF- $\kappa$ B gene expression (48, 57) or interleukin-8 production (49) in enterocytes, which are known effectors of TLR4 activation in monocytic cells (58, 59). However, these effects probably occur at later time points and under the regulation of signaling pathways different from Rho-GTPase activation, which may be very rapid (60). We postulate that the activation of a variety of signaling pathways by endotoxin determines the overall responsiveness of the enterocyte, and it is the precise control of these pathways that determines the ultimate effect of LPS after bacterial translocation has occurred.

The current study provides insights into how RhoA activation by LPS could inhibit intestinal epithelial restitution. Cell migration reflects the dynamic interaction between adhesion and deadhesion (61). Failure of cells to attach to the matrix results in lack of movement, whereas cells that attach too tightly cannot be released from the matrix and remain stationary (50). Sites of adherence occur through focal adhesions, which form in response to the activity of focal adhesion kinase under the regulation of RhoA (27, 51). Cell migration therefore

requires the down-regulation of RhoA, leading to the breakdown of stress fibers and loss of focal adhesions (8, 52, 62). In the current studies, we have shown that LPS increases RhoA activation in enterocytes, which leads to an increase in phospho-FAK expression and enhanced focal adhesions, as manifest by increased distribution of the focal adhesion protein paxillin (Fig. 7). This would effectively shift the balance toward enhanced cell contraction/adhesion and prevent cell movement. In support of this, we determined that enterocyte contraction is increased after LPS treatment compared with controls (Fig. 8) and could be reduced by inhibition of RhoA signaling using the Rho kinase inhibitor Y27632. Although this assay may be interpreted to reflect processes other than increased contraction, such as impaired release from the substratum or the generation of forces exerted by cell shape changes or intercellular adhesions, the results provide evidence that enterocytes adhere tighter to the matrix after LPS treatment (44). This could conceivably explain the impaired migration of enterocytes observed in response to LPS. This conclusion is further supported by evidence that endotoxin increases surface expression of integrins in enterocytes, which serve to directly enhance the enterocyte interaction with the underlying matrix.<sup>3</sup>

In summary, we have shown that epithelial restitution is impaired during experimental NEC, which provides insights into the pathogenesis of this disease. We have also demonstrated that endotoxin impairs enterocyte migration through the activation of RhoA, increased phospho-FAK expression, and enhanced cell matrix adhesion. This suggests that therapeutic approaches that target intestinal restitution, potentially by modulation of TLR4-mediated RhoA signaling, may provide a therapeutic approach for diseases of intestinal inflammation like NEC.

**Acknowledgments**—We thank Jun Li for expert technical assistance; Dr. Sergio Grinstein for ongoing advice and critical review of the manuscript; Drs. Ora Weisz, Thomas Kleyman, Alan Wells, David Perlmutter, Jeffrey Upperman, Anatoly Grishin, Faisal Qureshi, Ruben Zamora, Richard Simmons, and Timothy Billiar for advice, reagents, and constructive criticism; Dr. Nick Johnson for the generous gift of cortical collecting duct cells; and Patricia Boyle, Catey Wong, Giovanni Ruiz, Raul Rojas, Edward Wang, and Jey-Myung Lee for advice and support.

#### REFERENCES

- Guthrie, S. O., Gordon, P. V., Thomas, V., Thorp, J. A., Peabody, J., and Clark, R. H. (2003) *J. Perinatol.* **23**, 278–285
- Kafetzis, D. A., Skevaki, C., and Costalos, C. (2003) *Curr. Opin. Infect. Dis.* **16**, 349–355
- Berseth, C. L., Bisquera, J. A., and Paje, V. U. (2003) *Pediatrics* **111**, 529–534
- Noerr, B. (2003) *Adv. Neonatal Care* **3**, 107–120
- Atabai, K., Ishigaki, M., Geiser, T., Ueki, I., Matthay, M. A., and Ware, L. B. (2002) *Am. J. Physiol.* **283**, L163–L169
- Halpern, M. D., Holubec, H., Dominguez, J. A., Meza, Y. G., Williams, C. S., Ruth, M. C., McCuskey, R. S., and Dvorak, B. (2003) *Am. J. Physiol.* **284**, G695–G702
- Potoka, D. A., Nadler, E. P., Upperman, J. S., and Ford, H. R. (2002) *World J. Surg.* **26**, 806–811
- Horwitz, A. R., and Parsons, J. T. (1999) *Science* **286**, 1102–1103
- Nieuwenhuijzen, G., Deitch, E., and Goris, R. J. (1996) *J. Anat.* **189**, 537–548
- Tracey, K. J. (2002) *Nature* **420**, 853–859
- Amer, M. D., Hedlund, E., Rochester, J., and Caplan, M. S. (2004) *Biol. Neonate* **85**, 159–166
- Chen, L. W., Egan, L., Li, Z. W., Greten, F. R., Kagnoff, M. F., and Karin, M. (2003) *Nat. Med.* **9**, 575–581
- Ewer, A. K., Al-Salti, W., Coney, A. M., Marshall, J. M., Ramani, P., and Booth, I. W. (2004) *Gut* **53**, 207–213
- Mammen, J. M., and Matthews, J. B. (2003) *Crit. Care Med.* **31**, S532–S537
- Basson, M. D. (2001) *Life Sci.* **69**, 3005–3018
- Dignass, A. U. (2001) *Inflamm. Bowel Dis.* **7**, 68–77
- Podolsky, D. K. (1999) *Am. J. Physiol.* **277**, G495–G499
- Hackam, D. J., and Ford, H. R. (2002) *Surg. Infect.* **3**, Suppl. 1, 23–35
- Han, X., Fink, M. P., Yang, R., and Delude, R. L. (2004) *Shock* **21**, 261–270
- Mishima, S. M. D., Xu, D. M. D., Lu, Q. M. D., and Deitch, E. A. M. D. (1997) *Arch. Surg.* **132**, 1190–1195

<sup>2</sup> S. Cetin, F. Qureshi, J. Li, H. Ford and D. J. Hackam, manuscript in preparation.

<sup>3</sup> F. Qureshi, J. Li, H. Ford, and D. J. Hackam, manuscript in preparation.

21. De Plaen, I. G., Qu, X. W., Wang, H., Tan, X. D., Wang, L., Han, X. B., Rozenfeld, R. A., and Hsueh, W. (2002) *Immunology* **106**, 577–583
22. Forsythe, R. M., Xu, D. Z., Lu, Q., and Deitch, E. A. (2002) *Shock* **17**, 180–184
23. Longo, W. E., Damore, L. J., Mazuski, J. E., Smith, G. S., Panesar, N., and Kaminski, D. L. (1998) *Mediators Inflamm.* **7**, 85–91
24. Wang, Q., Wang, J. J., Boyce, S., Fischer, J. E., and Hasselgren, P.-O. (1998) *J. Surg. Res.* **76**, 27–31
25. Bochkov, V. N., Kadl, A., Huber, J., Gruber, F., Binder, B. R., and Leitinger, N. (2002) *Nature* **419**, 77–81
26. Le Roy, D., Di Padova, F., Adachi, Y., Glauser, M. P., Calandra, T., and Heumann, D. (2001) *J. Immunol.* **167**, 2759–2765
27. Hall, A. (1998) *Science* **279**, 509–514
28. Ridley, A. J. (2001) *Trends Cell Biol.* **11**, 471–477
29. Santos, M. F., McCormack, S. A., Guo, Z., Okolicany, J., Zheng, Y., Johnson, L. R., and Tigyi, G. (1997) *J. Clin. Invest.* **100**, 216–225
30. Akira, S., Takeda, K., and Kaisho, T. (2001) *Nat. Immunol.* **2**, 675–680
31. Lemaitre, B., Nicolas, E., Michaut, L., Reichhart, J. M., and Hoffmann, J. A. (1996) *Cell* **86**, 973–983
32. Hornef, M. W., Frisan, T., Vandewalle, A., Normark, S., and Richter-Dahlfors, A. (2002) *J. Exp. Med.* **195**, 559–570
33. Potoka, D. A., Upperman, J. S., Zhang, X. R., Kaplan, J. R., Corey, S. J., Grishin, A., Zamora, R., and Ford, H. R. (2003) *Am. J. Physiol.* **285**, G861–G869
34. Hackam, D., Rotstein, O., Sjolín, C., Schreiber, A., Trimble, W., and Grinstein, S. (1998) *Proc. Natl. Acad. Sci. U.S.A.* **95**, 11691–11696
35. Renshaw, M. W., Toksoz, D., and Schwartz, M. A. (1996) *J. Biol. Chem.* **271**, 21691–21694
36. Ren, X. D., Kiosses, W. B., and Schwartz, M. A. (1999) *EMBO J.* **18**, 578–585
37. O'Connor, K. L., Nguyen, B. K., and Mercurio, A. M. (2000) *J. Cell Biol.* **148**, 253–258
38. Hackam, D., Rotstein, O., Zhang, W., Demaurex, N., Woodside, M., Tsai, O., and Grinstein, S. (1997) *J. Biol. Chem.* **272**, 29810–29820
39. Hackam, D., Rotstein, O., Schreiber, A., Zhang, W., and Grinstein, S. (1997) *J. Exp. Med.* **186**, 955–966
40. Lavelle, J., Meyers, S., Ramage, R., Bastacky, S., Doty, D., Apodaca, G., and Zeidel, M. L. (2002) *Am. J. Physiol.* **283**, F242–F253
41. Nadler, E. P., Dickinson, E., Knisely, A., Zhang, X. R., Boyle, P., Beer-Stolz, D., Watkins, S. C., and Ford, H. R. (2000) *J. Surg. Res.* **92**, 71–77
42. Houle, V. M., Park, Y. K., Laswell, S. C., Freund, G. G., Dudley, M. A., and Donovan, S. M. (2000) *Pediatr. Res.* **48**, 497–503
43. Grinnell, F., Ho, C. H., Lin, Y. C., and Skuta, G. (1999) *J. Biol. Chem.* **274**, 918–923
44. Campbell, B. H., Clark, W. W., and Wang, J. H. (2003) *J. Biomech.* **36**, 137–140
45. Medvedev, A. E., and Vogel, S. N. (2003) *J. Endotoxin Res.* **9**, 60–64
46. Kjoller, L., and Hall, A. (1999) *Exp. Cell Res.* **253**, 166–179
47. Sachdev, P., Zeng, L., and Wang, L. H. (2002) *J. Biol. Chem.* **277**, 17638–17648
48. Abreu, M. T., Arnold, E. T., Thomas, L. S., Gonsky, R., Zhou, Y., Hu, B., and Arditi, M. (2002) *J. Biol. Chem.* **277**, 20431–20437
49. Suzuki, M., Hisamatsu, T., and Podolsky, D. K. (2003) *Infect. Immun.* **71**, 3503–3511
50. Larsen, M., Tremblay, M., and Yamada, K. (2003) *Nat. Rev. Mol. Cell. Biol.* **4**, 700–711
51. Parsons, J., Martin, K., Slack, J., Taylor, J., and Weeda, S. (2000) *Oncogene* **19**, 5606–5613
52. Rottner, K., Hall, A., and Small, J. V. (1999) *Curr. Biol.* **9**, 640–648
53. Duffy, L. C., Zielezny, M. A., Carrion, V., Griffiths, E., Dryja, D., Hilty, M., Cummings, J., and Morin, F. (2001) *Adv. Exp. Med. Biol.* **501**, 519–527
54. Bury, R. G., and Tudehope, D. (2001) *Cochrane Database Syst. Rev.* **1**, CD000405
55. Mercer, B. M., Miodovnik, M., Thurnau, G. R., Goldenberg, R. L., Das, A. F., Ramsey, R. D., Rabello, Y. A., Meis, P. J., Moawad, A. H., Iams, J. D., Van Dorsten, J. P., Paul, R. H., Bottoms, S. F., Merenstein, G., Thom, E. A., Roberts, J. M., and McNellis, D. (1997) *J. Am. Med. Assoc.* **278**, 989–995
56. Cario, E., Rosenberg, I. M., Brandwein, S. L., Beck, P. L., Reinecker, H.-C., and Podolsky, D. K. (2000) *J. Immunol.* **164**, 966–972
57. Abreu, M. T., Vora, P., Faure, E., Thomas, L. S., Arnold, E. T., and Arditi, M. (2001) *J. Immunol.* **167**, 1609–1616
58. Takeda, K., and Akira, S. (2004) *Semin. Immunol.* **16**, 3–9
59. Beutler, B., Hoebe, K., Du, X., and Ulevitch, R. J. (2003) *J. Leukocyte Biol.* **74**, 479–485
60. Hirabayashi, T., and Saffen, D. (2000) *Eur. J. Biochem.* **267**, 2525–2532
61. Ridley, A. J. (2001) *J. Cell Sci.* **114**, 2713–2722
62. Burrige, K. (1999) *Science* **283**, 2028–2029